Identification of polar nanoclusters in $PbMg_{1/3}Nb_{2/3}O_3$ from NMR spectra

M. Vijayakumar,[1] Gina L. Hoatson,[1,*] and Robert L. Vold[2]
[1]*Department of Physics, College of William and Mary, P.O. Box 8795, Williamsburg, Virginia 23187-8795, USA*
[2]*Department of Applied Science, College of William and Mary, P.O. Box 8795, Williamsburg, Virginia 23187-8795, USA*
(Received 10 August 2006; revised manuscript received 13 November 2006; published 8 March 2007)

Nuclear magnetic resonance (NMR) spectra of ^{93}Nb in the ferroelectric relaxor, lead magnesium niobate, have been obtained as a function of temperature, from 200 K to 370 K, at 17.6 T with magic angle spinning at 30 kHz. The central transition region consists of three overlapping peaks, and deconvolution yields temperature-dependent distributions of isotropic chemical shift (δ_{iso}^{cs}) and quadrupole coupling parameters (C_Q, η_Q) for each peak. Variable-temperature multiple quantum magic angle spinning (MAS) experiments confirm the accuracy of the procedures used to fit MAS spectra. The three peaks have been assigned to Nb^{5+} cations with specific configurations of next-nearest B-site neighbors (nBn) in the perovskite structure. Analysis of the temperature dependence provides the first unambiguous observation of specific local nBn structures associated with the polar nanoclusters. At temperatures below the Burns temperature, T_B=620 K, but well above the onset of macroscopic remnant polarization (270 K), the polar nanoclusters have only zero or one Mg^{2+} ion in the nBn shell. As the temperature decreases, the cooperative ferroelectric distortion characteristic of polar nanoclusters accommodates configurations with progressively more Mg^{2+} nBn ions. Effectively, each specific configuration has a different transition temperature, which explains the observed relaxor behavior.

DOI: 10.1103/PhysRevB.75.104104 PACS number(s): 77.84.Dy, 82.56.Ub, 82.56.Fk

INTRODUCTION

Lead magnesium niobate, $PbMg_{1/3}Nb_{2/3}O_3$ (PMN), is a high-performance relaxor ferroelectric that is used extensively in technological applications including ultrasonic transducers, electromechanical switches, and actuators.[1–3] In contrast to normal ferroelectric materials, the paraelectric to ferroelectric transition in relaxors is diffuse: on lowering the temperature the bulk remnant polarization rises continuously, and the temperature of maximum dielectric permeability, T_m, is frequency dependent.[2] It is generally agreed that both structural and chemical disorder play crucial roles in relaxor behavior.[2,4] The generally accepted physical picture is one of nanoclusters (spanning at least a few unit cells) in which local electric dipole moments are aligned, dispersed in a neutral matrix. These "polar nanoclusters" begin to form at the Burns temperature, T_B. Original optical measurements,[5] confirmed by more recent x-ray and neutron diffraction experiments,[3] show that for PMN, $T_B \sim 620$ K. However, the temperature of maximum permittivity in PMN is much lower, T_M=270 K. Improving the understanding of the microscopic origin of the macroscopic properties of relaxors is of central importance to the fundamental theory of ferroelectric behavior and may also provide insights for the development of new materials whose physical properties can be optimized for specific applications.

Several models have been proposed to relate the local, microscopic polarization to the gradual onset of macroscopic polarization, including superparaelectric glasses,[6] dipole glasses,[7] and random bond-random field interactions.[8] The microscopic identity of the polar nanoclusters is not specified in any of these models and cannot be determined from measurements of bulk physical properties such as dielectric permeability or dipole moment. Clearly, a more specific local probe is required. Solid-state NMR is ideal for this purpose, because the relevant NMR parameters (chemical shifts and electric field gradient tensors for quadrupolar nuclei) are sensitive to the immediate environment of identifiable atomic nuclei. Very recent measurements of the temperature and electric field dependence of static ^{207}Pb NMR spectra of PMN show that at low temperature (40 K), about 50% of the lead ions reside in "frozen polar clusters," whose polarization can orient in response to a strong electric field.[9] This result is consistent with a recent analysis of neutron pair distribution functions of PMN,[10] in which polar nanoclusters were modeled in terms of a fraction, α, of rhombohedral units in which B-site ions (Mg/Nb) are displaced along the local ⟨111⟩ direction. However, the precise, atomic-level identity of polar nanoclusters remains elusive.

In PMN, the B sites in the ABO_3 perovskite lattice are occupied by Nb^{5+} and Mg^{2+} cations in 2:1 ratio, and are surrounded by an octahedral shell of six O^{2-} ions. Each Nb^{5+} cation has six nearest-neighbor B sites, which can be occupied by either Nb^{5+} or Mg^{2+}, with probability consistent with the overall 2:1 stoichiometry. X-ray diffuse scattering and neutron diffraction studies[3] suggested, and solid-state NMR experiments[11] proved, that the random site model[12] provides the best description of short-range disorder. Ordered domains exist along the ⟨111⟩ direction, with alternate B-ion layers consisting exclusively of Nb^{5+} interleaved with randomly mixed Nb^{5+} or Mg^{2+} cations (in 1:2 ratio to ensure the correct overall stoichiometry). In pure PMN, this short-range order does not extend beyond a few unit cells, even after prolonged thermal annealing of single-crystal samples. In contrast, ordered domains extending up to ~300 nm exist in carefully annealed solid solutions of PMN and lead scandium niobate $PbSc_{1/2}Nb_{1/2}O_3$ (PSN)[12] (for x=0.6).

In previous papers, we showed that high-field ^{93}Nb NMR MAS and three quantum MAS (3QMAS) experiments can be used to quantitatively identify specific configurations of next-nearest B-site neighbor (nBn) cations.[11,13] In this paper, we analyze the temperature dependence of ^{93}Nb MAS and

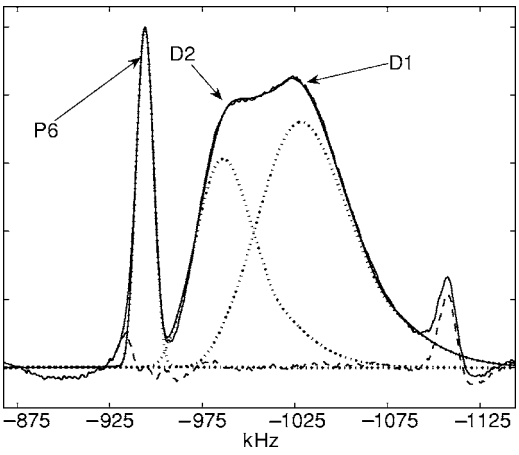

FIG. 1. ^{93}Nb MAS NMR spectrum of PMN at $T=350$ K, $\nu_R=30$ kHz, and 17.6 T (183.4 MHz). Dotted lines are simulated peaks P6, D1, and D2, computed with Gaussian distributions of isotropic chemical shift and quadrupole coupling constants. The sharp line near −1100 ppm is a sideband and was not included in the simulation. Best-fit parameters for peak P6 are $\delta_{iso}^{cs}=-902$ ppm (relative to saturated $NbCl_5$ in acetonitrile) with Gaussian distribution width (one std. dev.) $\sigma_{CS}=3.0$ ppm; $C_Q=8.5$ MHz with distribution width $\sigma_Q=0.5$ MHz; and relative (integrated) intensity $A=13.4\%$. For D1 the corresponding parameters are $\delta_{iso}^{cs}=-973.6$ ppm, $\sigma_{CS}=14.4$ ppm; $C_Q=28$ MHz, $\sigma_Q=5.2$ MHz; and $A=54.7\%$ and for D2, $\delta_{iso}^{cs}=-938$ ppm, $\sigma_{CS}=9.3$ ppm, $C_Q=24$ MHz, $\sigma_Q=4$ MHz, and $A=31.2\%$.

three quantum MAS (3QMAS) spectra to discover which specific nBn configurations form polar nanoclusters in PMN. Earlier investigations[14] at lower magnetic fields lacked sufficient resolution to achieve this.

EXPERIMENTAL METHODS

A ^{93}Nb MAS NMR spectrum of PMN obtained at 17.6 T with spin rate 30 kHz is shown in Fig. 1. The central transition region consists of three partially resolved lines and is accompanied by manifolds of spinning sidebands arising from satellite transitions. The sharp peak (P6) is assigned to Nb^{5+} ions in the highly symmetric environment consisting of six Mg^{2+} nBn ions; distribution peak D1 arises from niobium ions with zero or one Mg^{2+} nBn ions; and distribution peak D2 arises from niobium with 2–5 Mg^{2+} nBn ions. These assignments are nontrivial and are based on a careful analysis of MAS and 3QMAS spectra of a series of $(1-x)$ PMN xPSN solid solutions with mole fraction PSN $x=0$, 0.1, 0.2, 0.6, 0.7, and 0.9.[11]

The central transition frequency of each Nb^{5+} site is determined by three parameters: the isotropic chemical shift, δ_{iso}^{cs}, the quadrupole coupling constant, C_Q, and the asymmetry parameter, η_Q, of the electric field gradient tensor. In disordered materials, the central transition lacks the sharp edges and singularities observed in simple crystalline materials. Therefore, it is necessary to fit the line shapes for P6, D1, and D2 using distributions of both isotropic chemical shifts and quadrupole coupling constants. In principle, the line shape of each peak is determined by seven parameters: its (integrated) relative intensity, the mean values of δ_{iso}^{cs}, C_Q, and η_Q, and the corresponding widths σ_{CS}, σ_Q, and σ_η. In the spectral deconvolution presented in this communication, η was fixed to values determined by previous 3QMAS measurements at 19.6 T:[11] $\eta_Q=0.99$ for P6 and $\eta_Q=0.5-0.6$ for D1 and D2. This reduces the number of variable parameters for each peak from seven to five. Introducing such constraints is essential to reliable deconvolution of the spectra and the accuracy of the fitted parameters.

Since the transition frequency depends linearly on the isotropic chemical shift, a Gaussian distribution of δ_{iso}^{cs} must produce a symmetric, Gaussian line shape. However, the quadratic dependence of transition frequency on quadrupole coupling constant implies that a symmetric, Gaussian distribution of C_Q itself produces a characteristically asymmetric line shape. This effect, which becomes noticeable when the distribution width is more than about 10% of the mean value, is clearly visible in the line shapes needed to fit the D1 and D2 peaks. The best fit MAS line shapes shown in Fig. 1 were obtained by visual adjustment of the relevant parameters to yield minimum residuals and could not be reproduced by any physically reasonable superposition of symmetric Gaussian or Lorentzian components.

It is difficult to obtain reliable independent values for the two distribution widths by fitting overlapping MAS spectra at a single magnetic field. Validation of the procedure used in this paper to fit MAS spectra is provided by 3QMAS experiments.[11] The triple and single quantum frequencies in a 3QMAS experiment are given (in ppm) by

$$\upsilon_1 = 3\delta_{iso}^{cs} + \frac{3P_Q^2}{10\upsilon_L^2}C_0(3/2,I) + 20\frac{\upsilon_Q^2}{\upsilon_L^2}F_4(\alpha,\beta,\eta)C_4(3/2,I), \tag{1a}$$

$$\upsilon_2 = \delta_{iso}^{cs} + \frac{3P_Q^2}{10\upsilon_L^2}C_0(1/2,I) + 20\frac{\upsilon_Q^2}{\upsilon_L^2}F_4(\alpha,\beta,\eta)C_4(1/2,I). \tag{1b}$$

Here, I is the spin quantum number ($I=9/2$ for ^{93}Nb), and the quadrupole product is defined as $P_Q=(1+\eta^2/3)\upsilon_Q$, where $\upsilon_Q=C_Q/2I(2I-1)$ and C_Q is the quadrupole coupling constant.[11] The angular factors $F_4(\alpha,\beta,\eta)$ depend on crystallite orientation angles α and β as well as the electric field gradient asymmetry parameter, η. Expressions for $F_4(\alpha,\beta,\eta)$ and the coefficients C_0 and C_4 may be found in the literature.[11] It is customary to process 3QMAS spectra using a shearing transformation: frequencies on the horizontal axis (direct dimension, υ_2) are then given by Eq. (1b), while frequencies on the vertical axis (indirect dimension, υ_1) are given by a modified formula, $\upsilon_1'=\upsilon_1-k\upsilon_2$, where the shear factor k is an arbitrary constant. In the original literature on 3QMAS experiments,[15] $k=C_4(3/2,I)/C_4(1/2,I)$ was used to suppress second-order quadrupole broadening caused by the F_4 term. For PMN and other disordered systems, it is often more useful to choose $k=3$. This does not fully eliminate quadrupole broadening, but it does eliminate all effects of δ_{iso}^{cs} from one-dimensional slices parallel to the υ_1 axis. Thus,

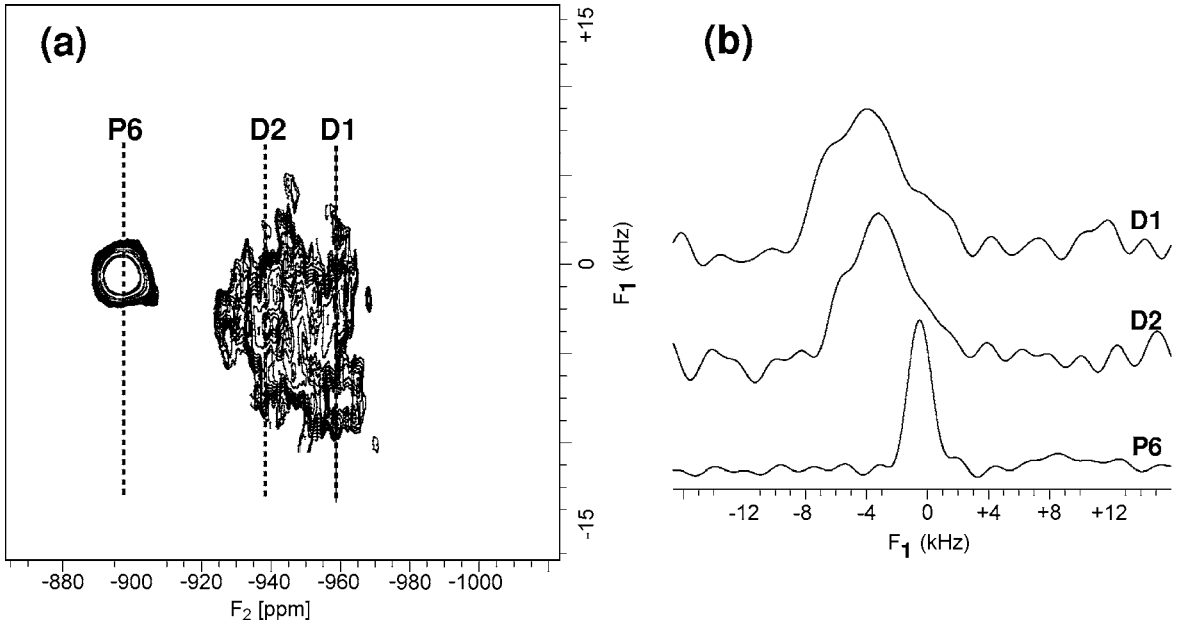

FIG. 2. ^{93}Nb MAS 3QNMR spectrum of PMN at $T=350$ K, $\nu_R=30$ kHz, and 17.6 T (183.4 MHz). The contour plot (a) was obtained with shear factor of 3. For reasons discussed in the text, the line shapes along F1 corresponding to MAS peaks P6, D1, and D2, shown in (b), are therefore determined by the quadrupole coupling parameters alone.

peak positions along υ_1 are independent of any chemical shift parameters and their distribution.

A two-dimensional triple quantum MAS spectrum of PMN obtained at 17.6 T and 350 K, sheared with $k=3$, is shown in Fig. 2(a). Slices along υ_1 corresponding to the υ_2 peak positions of P6, D1, and D2 are shown in Fig. 2(b). The slice corresponding to peak P6 is consistent with a small mean value of the quadrupole coupling constant, $C_Q=8.5$ MHz, with a narrow distribution, $\sigma_Q=0.5$ MHz. The line shape for D2, which is composed of asymmetric nBn configurations with 1–4 Nb^{+5} cations, has a broad distribution ($\sigma_Q=4$ MHz) centered at the relatively large value, $C_Q=24$ MHz. The slice for D1 shows a wider distribution with both small ($C_Q\sim 6-8$ MHz) and large ($C_Q\sim 30-35$ MHz) values. This is consistent with its assignment to an overlapping sum of two nBn configurations with five Nb^{+5} cations (asymmetric, large C_Q) and six Nb^{5+} cations (symmetric, smaller C_Q). Mean quadrupole coupling constants estimated from the υ_1 slices of 3QMAS spectra were used as starting values for fitting the line shapes of one-dimensional (1D) MAS spectra, and agree, within experimental error, with the final best fit values. The intensities of multiple quantum spectra are invariably distorted due to efficient excitation of 3Q coherence for large quadrupolar coupling constants and pulse artifacts, and thus these were not used for quantitative analysis.

RESULTS AND DISCUSSION

The temperature dependences of the best-fit parameters are shown in Figs. 3–5. C_Q for peak P6 [solid triangles, Fig. 3(a)] shows only a small increase with decreasing temperature, as expected for reduced amplitudes of lattice vibration.[16] The chemical shift of this peak is also essentially independent of temperature [Fig. 3(b)]. The temperature dependences of C_Q and δ_{iso}^{cs} for peak D2 (open circles) also show at most small, monotonic changes. However, for peak D1, both C_Q and especially δ_{iso}^{cs} show significantly stronger temperature dependence. Interestingly, the distribution widths for C_Q [Fig. 4(a)] and δ_{iso}^{cs} [Fig. 4(b)] of D1 both *decrease* with decreasing temperature: for C_Q, the distribution width drops smoothly from 5.6 MHz at 373 K to a constant value ~3 MHz below 270 K, and for δ_{iso}^{cs} the distribution width remains constant until 270 K, where it, too, begins to decrease. The relative intensity of P6 is independent of temperature within experimental error, but counterintuitively, peak D1 gains intensity at the expense of D2 as temperature decreases (Fig. 5). However, there is no observable discontinuity around the nominal paraelectric-ferroelectric phase transition at $T=270$ K.

Off-centering of a central Nb^{5+} cation with respect to its surrounding oxygen octahedron must produce a large local electric dipole moment and electric field gradient. The associated changes in Nb-O distances and bond angles must also affect both C_Q and δ_{iso}^{cs}. Point charge models of the electric field gradient imply that the loss of symmetry due to off-centering should increase C_Q by a factor proportional to $1/\Delta r^3$, where Δr is the displacement of the central Nb^{5+} cation. Thus, the strong temperature dependence observed for C_Q in peak D1 implies that off-centering of Nb^{5+} in configurations with either zero or one Mg^{2+} nBn cations is larger than in configurations with two or more Mg^{2+} nBn cations. Presumably, this occurs because there is more "free volume" in the oxygen octahedra for configurations with more smaller ions (the ionic radii of Nb^{5+} and Mg^{2+} are 0.64 and 0.72 Å, respectively). The large number (5 or 6) of small, highly charged Nb^{5+} ions in these configurations also results in large, local dipole moments. Predicting the effect of off-

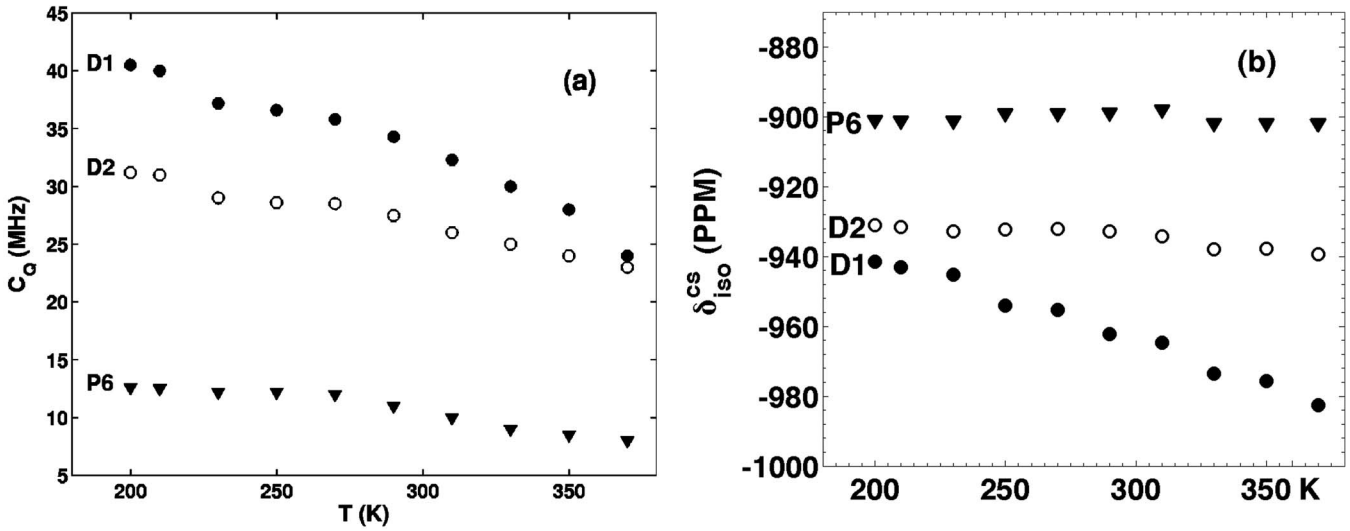

FIG. 3. Temperature dependence of C_Q (a) and δ^{cs}_{iso} (b) for P6 (triangles), D1 (closed circles), and D2 (open circles). The strong temperature dependence observed for D1 implies larger displacements of Nb^{5+} cations in B-site configurations with at most one Mg^{2+} nBn cation.

centering on δ^{cs}_{iso} is more difficult and would require accurate *ab initio* chemical shift calculations.

The distribution of displacements of Nb^{5+} cations in polar nanoclusters should be narrower than for those in the surrounding, inert spin-glass matrix, because displacements in spatially proximate unit cells must produce parallel local dipole moments. Thus, the decrease in C_Q and δ^{cs}_{iso} distribution widths, σ_Q and σ_{CS}, observed for peak D1 near the paraelectric to ferroelectric phase transition at 270 K implicates configurations with either zero or one Mg^{2+} nBn cation as the most favorable local structures for formation of polar nanoclusters.

The observation that peak D1 grows at the expense of D2 with decreasing temperature is consistent with recent ^{207}Pb NMR results on PMN,[9] and with recent high-energy x ray diffuse scattering measurements on $Pb(Zn_{1/3}Nb_{2/3})O_3$.[17] Over the temperature range of the present study, 200–373 K, the relative populations of the various nBn configurations cannot possibly change; B-site ions are not free to exchange from site to site. Instead, the polar nanoclusters are dynamic: the observed (mean) C_Q and δ^{cs}_{iso} values reflect an average over the thermally accessible range of lattice distortions. Thus, the temperature-independent NMR parameters found for P6 indicate that unit cells with six Mg^{2+} cations are entirely excluded from the polar nanoclusters. As temperature decreases polar nanoclusters associated with peak D1 increase in size. When they encounter unit cells with more than one Mg^{2+} cation, a local ferroelectric distortion (Nb^{5+} cation off-centering) is induced that shifts the time-averaged NMR parameters from those characteristic of D2 to those charac-

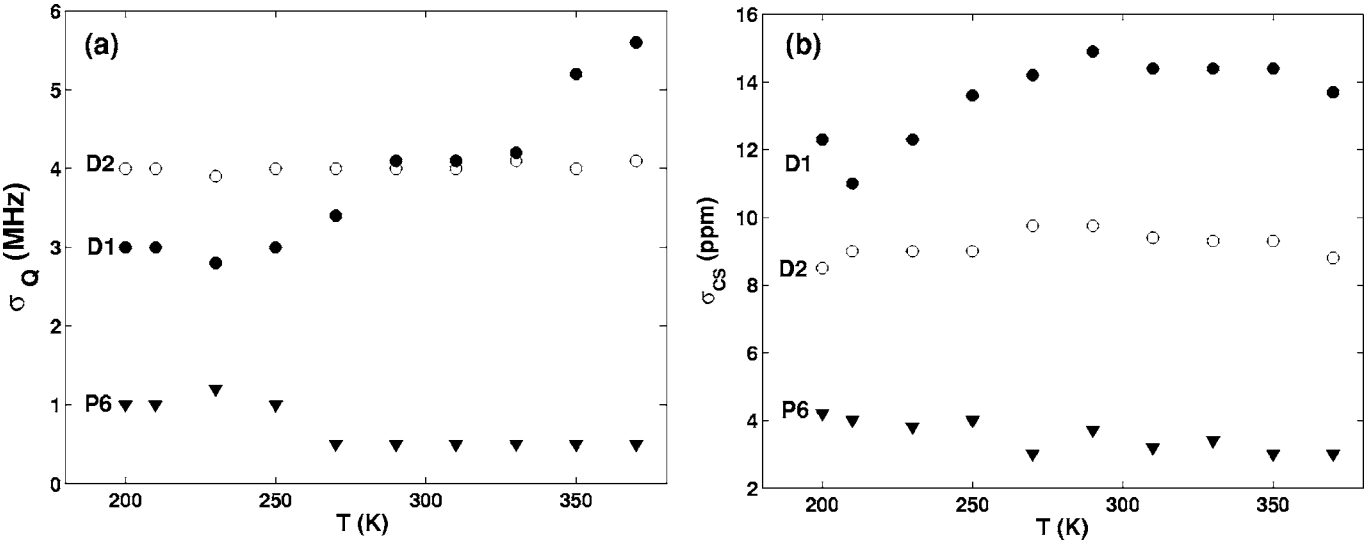

FIG. 4. Temperature dependence of Gaussian distribution widths for C_Q (a) and δ^{cs}_{iso} (b) of P6 (triangles), D1 (closed circles), and D2 (open circles). For reasons outlined in the text, the decreased distribution widths found at low temperature for D1 implicates Nb^{5+} B-site configurations with at most one Mg^{2+} nBn cation as the origin of polar nanoclusters.

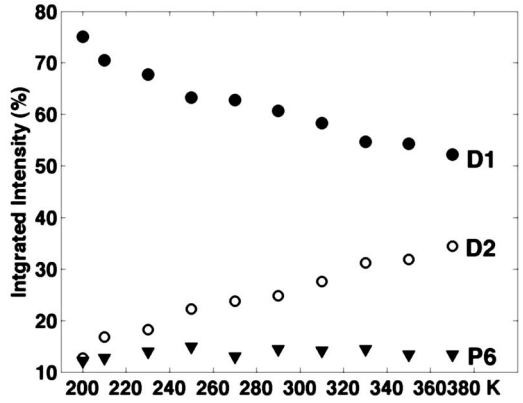

FIG. 5. Relative (integrated) intensities of peaks P6 (triangles), D1 (closed circles), and D2 (open circles). P6 does not contribute to polar nanoclusters. See text for an explanation of how the intensities can change with temperature, even though the B-site occupation probabilities cannot.

teristic of D1. In effect, the transition temperature of local domains depends on the number of nBn Mg^{2+} ions: as the temperature is decreased, niobium ions in nBn configurations with progressively more Mg^{2+} cations move off-center and become part of the cooperative polar nanoclusters.

CONCLUSIONS

High-field, variable-temperature ^{93}Nb NMR spectra of the ferroelectric relaxor PMN have been used to assign different lines to specific nBn configurations. The distribution peak, D1, has been interpreted in terms of the growth of polar nanoclusters with decreasing temperature. Local structures, in which a central Nb^{+5} cation is surrounded by six next-nearest B-site neighbor Mg^{2+} ions, do not participate in the polar nanoclusters. Polar nanoclusters in PMN have no unique local structure. Instead, they consist of spatially proximate unit cells with a highly nonrandom set of niobium nBn configurations, and the nBn configurations that participate depend on temperature. At temperatures well above T_m, polar nanoclusters have zero or one Mg^{2+} ion in the nBn shell. As the temperature decreases, the cooperative ferroelectric distortion characteristic of polar nanoclusters accommodates configurations with progressively more Mg^{2+} nBn ions. Effectively, each specific configuration has a different transition para- to ferroelectric transition temperature that explains the observed relaxor behavior.

ACKNOWLEDGMENTS

This work was supported by the Office of Naval Research, Grant N000140310661, and the National Science Foundation, Grant CHE0079136. We thank Peter Davies (University of Pennsylvania) for many useful discussions and for providing PMN samples. The high-field NMR spectrometer was funded by equipment grants from the NSF MRI Program, CHE 0216200, the Office of Naval Research ONR N00014-02-1-0669 (DURIP), and the College of William and Mary.

*Author to whom correspondence should be addressed: gina@physics.wm.edu

[1] Z.-G. Ye, Key Eng. Mater. **155-6**, 81 (1998).
[2] L. E. Cross, Ferroelectrics **151**, 305 (1994).
[3] P. Bonneau, P. Garnier, G. Calvarin, E. Husson, J. R. Gavarri, A. W. Hewat, and A. Morell, J. Solid State Chem. **91**, 350 (1991).
[4] I. W. Chen, J. Phys. Chem. Solids **61**, 197 (2000).
[5] G. Burns and F. H. Dacol, Solid State Commun. **48**, 853 (1983).
[6] L. E. Cross, Ferroelectrics **76**, 241 (1987); D. Viehland, J. F. Li, S. J. Jang, L. E. Cross, and M. Wuttig, Phys. Rev. B **43**, 8316 (1991).
[7] E. V. Colla, E. Y. Koroleva, N. M. Okuneva, and S. B. Vakhrushev, Phys. Rev. Lett. **74**, 1681 (1995).
[8] R. Pirc and R. Blinc, Phys. Rev. B **60**(19), 13470 (1999).
[9] R. Blinc, V. V. Laguta, V. Zalar, and J. Banys, J. Mater. Sci. **41**, 27 (2006).
[10] I.-K. Jeong, T. W. Darling, J. K. Lee, T. Proffen, R. H. Heffner, J. S. Park, K. S. Hong, W. Dmowski, and T. Egami, Phys. Rev. Lett. **94**, 147602 (2005).
[11] D. H. Zhou, G. L. Hoatson, and R. L. Vold, J. Magn. Reson. **167**, 242 (2004).
[12] M. A. Akbas and P. K. Davies, J. Am. Ceram. Soc. **80**, 2933 (1997).
[13] G. L. Hoatson, D. H. Zhou, F. Fayon, D. Massiot, and R. L. Vold, Phys. Rev. B **66**, 224103 (2002).
[14] M. D. Glinchuk, V. V. Laguta, I. P. Bykov, S. Nokhrin, V. P. Botvun, M. A. Leschenko, J. Rosa, and L. Jastrabik, J. Appl. Phys. **81**, 3561 (1997); J. J. Fitzgerald, J. Huang, and J. S. Shore, Ferroelectrics **233**, 187 (1999); V. V. Laguta, M. D. Glinchuk, S. N. Nokhrin, I. P. Bykov, R. Blinc, A. Gregorovic, and B. Zalar, Phys. Rev. B **67**, 104106 (2003).
[15] L. Frydman and J. S. Harwood, J. Am. Chem. Soc. **117**, 5367 (1995).
[16] H. Bayer, Z. Phys. **130**, 227 (1951).
[17] G. Xu, Z. Zhong, Y. Bing, Z.-G. Ye, and G. Shirane, Nat. Mater. **5**, 134 (2006).